Glycerol oxidation with gold supported on carbon xerogels: Tuning selectivities by varying mesopore sizes

Elodie G. Rodrigues, Manuel F.R. Pereira, José J.M. Órfão *

Laboratório de Catálise e Materiais (LCM), Laboratório Associado LSRE/LCM, Departamento de Engenharia Química, Faculdade de Engenharia, Universidade do Porto, Rua Dr. Roberto Frias, 4200-465 Porto, Portugal

ARTICLE INFO

ABSTRACT

Two carbon xerogels (CX) with different pore size distributions were prepared by the conventional approach (condensation of resorcinol and formaldehyde). The key variable to control those sizes is the pH of the aqueous solution. Gold nanoparticles were supported on the prepared CXs by the sol immobilization method and tested in the selective oxidation of glycerol, with the main purpose of evaluating the influence of the textural properties on the activity and selectivity. Mesopore sizes of the support have a strong effect on the distribution of products: wide pores enhance the formation of dihydroxyacetone whereas narrow mesopores favor the oxidation towards glyceric acid. Additionally, the selectivity results obtained with carbon xerogels were compared with those achieved with other carbon supports (activated carbon and multi-walled carbon nanotubes) and the same trend was observed. Therefore, it seems that the distribution of products can be controlled by the adequate choice of the support. For this purpose, carbon xerogel is a promising material since its pore size can be easily modified in a controllable way during the preparation stage.

© 2011 Elsevier B.V. All rights reserved.

1. Introduction

Over the last decade, biodiesel has emerged as a viable clean fuel. Nevertheless, its increasing global demand has created a major surplus of glycerol [1]. The valorization of this highly versatile molecule is a research area that has received tremendous attention in recent years, as glycerol is nontoxic, easily available, biodegradable and a potential starting material for numerous value-added chemicals [1,2].

Liquid phase catalytic oxidation is a promising route to convert glycerol into useful compounds, provided that the catalyst used is sufficiently active and selective for the formation of chemicals such as glyceric acid (GLYCEA) and/or dihydroxyacetone (DIHA), potentially useful as chemical intermediates in the fine chemicals industry, particularly in pharmaceuticals [1,2]. However, due to the high functionality of glycerol, a complex reaction pathway exists [2–4].

Platinum, palladium and rhodium catalysts have been described as highly active for the oxidation of glycerol in the liquid phase [5–8]. However, catalysts that are based on these metals deactivated at increasing reaction time due to oxygen poisoning [9,10]. On the other hand, gold has a better resistance to oxygen poisoning,

allowing for the use of higher oxygen partial pressures [11,12]. Nano-sized gold particles supported on different carbon materials (e.g. carbon black, activated carbon and graphite) and oxides (TiO$_2$, MgO and Al$_2$O$_3$) are active for the oxidation of glycerol but show very different performances, carbon supported gold catalysts being more active than most oxides supported catalysts [11,13,14]. Moreover, an increasing number of studies suggest that textural and chemical properties of the support influence directly the selectivity of the process [15–18]. Recently, we reported that the use of multi-walled carbon nanotubes as support for Au nanoparticles results in the preferential oxidation of the secondary hydroxyl group and subsequent formation of DIHA; on the other hand, an activated carbon supported gold catalyst, with similar metal content and average particle size, promotes the formation of glyceric acid [18]. It was suggested that the peculiar porous characteristics of MWCNTs, including the presence of large mesopores, may favor the oxidation towards dihydroxyacetone due to a different adsorption mode. The same explanation was proposed by Prati et al. [17] when testing gold supported on carbon nanofibers for the oxidation of glycerol under base-free conditions. Therefore, it seems that the support textural properties, namely mesopore sizes, can be a key factor in order to tune the selectivity of catalysts. For this purpose, carbon xerogel (CX) is a promising material since its pore size distribution can be easily modified in a controllable way [19]. Until now, this material has not been investigated as support for gold nanoparticles in the scope of the liquid phase oxidation of glycerol. However, these polymer derived mesoporous carbon materials have been

* Corresponding author. Tel.: +351 225 081 665; fax: +351 225 081 449.
E-mail addresses: elodie.rodrigues@fe.up.pt (E.G. Rodrigues), fpereira@fe.up.pt (M.F.R. Pereira), jjmo@fe.up.pt (J.J.M. Órfão).

drawing increasing attention for catalytic applications since they possess high surface area, high porosity, high stability in acid and basic media, open pore network and controllable pore size [19]. A suitable support material is crucial for good catalytic activity and stability. Carbon materials are widely used since they present advantages as high stability in acidic and basic media. This feature is primordial in gold catalyzed glycerol oxidation since reactions are performed in a high pH medium [16,20,21]. Moreover, carbon supports offer the possibility of recovering precious metals by burning off spent catalysts. Therefore, CXs possess excellent characteristics as catalyst support.

In the present work, two mesoporous carbon xerogels having different pore sizes were prepared and used as support in the preparation of gold catalysts. Then, the prepared catalysts were evaluated in the liquid phase glycerol oxidation, in order to investigate the possible role of the mentioned property on the catalytic performance.

2. Experimental

2.1. Preparation procedures

Two carbon xerogels differing in their textural properties were synthesized. Subsequently, gold was supported on these materials by the sol immobilization method.

2.1.1. Preparation of carbon xerogels

Two carbon xerogels were prepared by the sol–gel condensation of resorcinol and formaldehyde at two different pHs (5.5 and 6.0), and subsequent carbonization of the dried gels, according to Job et al. [19].

In this procedure, 30 g of resorcinol were dissolved in 57 mL of distilled water under magnetic stirring. After dissolution the pH was about 3; then it was adjusted to a value close to the chosen one by the addition of 2 M NaOH aqueous solution. Subsequently, 40 mL of formaldehyde solution (37 wt%, containing 10–15 wt% MeOH) were added to the resorcinol solution under continuous stirring. The final pH value was then adjusted by addition of diluted sodium hydroxide solution (0.5 M). Stirring continued for 90 min, and then it was stopped, the magnetic bar was removed, and the content was left for 3 days in a shaker at 85 °C to perform the gelation. The hard gel formed was then ground and water was removed by drying in an air oven for a period of 7 days. The temperature was increased stepwise from 60 to 150 °C as following: 1st day at 60 °C, 2nd day at 80 °C, 3rd day at 100 °C, 4th day at 120 °C, and from 5th to 7th day at 150 °C. Mesoporous carbon samples were obtained by pyrolysis of the dried gels under nitrogen flow (100 cm^3 min^{-1}, STP) at 800 °C in a tubular furnace. The heating program included the following sequential steps: (1) ramp at 2 °C min^{-1} to 150 °C and hold for 60 min; (2) ramp at 2 °C min^{-1} to 400 °C and hold for 60 min; (3) ramp at 2 °C min^{-1} to 600 °C and hold for 60 min; (4) ramp at 2 °C min^{-1} to 800 °C and hold for 360 min; (5) cool slowly to room temperature. A shrinkage corresponding to approximately 50 wt% was observed after carbonization.

The carbon xerogels obtained were designated as 5CX (sol–gel processing at pH 6.0) and 20CX (sol–gel processing at pH 5.5). The numbers 5 and 20 correspond to the most frequent mesopore diameters of the samples (in nm), as it can be seen in Section 3.1.1. These materials were ground to a particle diameter between 0.1 and 0.3 mm before use, in order to avoid mass transfer resistance effects and facilitate the accessibility of reactants to gold active sites.

2.1.2. Preparation of catalysts

Catalyst samples were prepared via the sol immobilization technique, using polyvinyl alcohol (PVA) as protective agent and NaBH$_4$ as reducing agent [22]. Briefly, HAuCl$_4$·3H$_2$O (35.1 mg) was dissolved in 690 mL of H$_2$O, and PVA was added (1.6 mL, 0.2 wt%) under stirring. Then, NaBH$_4$ (4 mL, 0.1 M) was introduced in the yellow solution under vigorous magnetic stirring, leading to the generation of a ruby-red metallic sol. After a few minutes, the colloid was immobilized by adding the carbon xerogel under fast stirring. The amount of support was calculated in order to have a final gold loading of 1 wt% in the catalyst. When the solution became colorless, the suspension was filtered. The catalyst was washed thoroughly with distilled water until the filtrate was free of chloride (checked by the AgNO$_3$ test) and dried at 110 °C for 24 h.

The organic scaffold was removed by heat treatment under nitrogen flow for 3 h at 350 °C, and then the catalyst was activated by reduction under hydrogen flow for 3 h also at 350 °C.

This method typically provides nanoparticle sizes around 5–6 nm both in activated carbon and carbon nanotubes [12,18,22].

2.2. Characterization

Catalysts and supports were characterized by N$_2$ adsorption at −196 °C in a NOVA Quantachrome Instruments apparatus. BET surface area (S_{BET}), mesopore surface area (S_{meso}) and micropore volume (V_{micro}) were calculated using the BET equation and the t-method, respectively. Pore size distributions were obtained from the desorption branch of the isotherm using the Barrett, Joyner and Halenda (BJH) method.

The determination of oxygenated surface functional groups was performed by temperature programmed desorption–mass spectrometry (TPD–MS) [23,24]. CO and CO$_2$ TPD spectra were obtained with a fully automated AMI-200 equipment (Altamira Instruments). In a typical experiment, the sample (150 mg) was placed in a U-shaped quartz tube inside an electrical furnace and subjected to a 5 °C min^{-1} linear temperature increase up to 1100 °C under helium flow (25 cm^3 min^{-1}, STP). A quadrupole mass spectrometer (Dymaxion 200, Ametek) was used to monitor CO and CO$_2$ signals. For quantification of the CO and CO$_2$ released, calibration of these gases was carried out at the end of the analysis.

The gold loading of the prepared catalysts was determined in duplicate by inductively coupled plasma–optical emission spectroscopy (ICP/OES) in an external laboratory (CACTI Vigo, University of Vigo), using a PerkinElmer Optima 4300 DV spectrometer.

Electron micrographs of samples were obtained at CACTI Vigo, University of Vigo, using a JEOL 2010F instrument. Size distributions were determined by the measurement of more than 200 nanoparticles and the average diameter was calculated by $d_M = \sum d_i n_i / \sum n_i$, where n_i is the number of particles with diameter d_i.

2.3. Catalytic experiments

In standard tests, a NaOH solution and the gold catalyst (700 mg) were added to a 0.3 M aqueous solution of glycerol (total volume 195 mL; NaOH/glycerol molar ratio = 2) under stirring at 1000 rpm. The reactor was pressurized with nitrogen at 3 bar. After heating to 60 °C under this atmosphere, the reaction was initiated by switching from inert gas to oxygen (3 bar). The stirring speed of 1000 rpm was selected on the basis of preliminary experiments, which showed that external mass transfer limitations were overcome in these conditions.

The reaction was monitored by taking samples (0.5 mL) for analysis at regular time intervals. The quantitative analysis of the mixtures was carried out by high performance liquid chromatography (HPLC). The chromatograph (Elite LaChrom HITACHI) is equipped with an ultraviolet (210 nm) and a refractive index detector in series. Compounds were identified by comparison with standard samples and concentrations were calculated using calibration curves previously determined.

Table 1
Textural properties of supports and catalyst Au/20CX.

Sample	S_{BET} (m^2 g^{-1})	S_{meso} (m^2 g^{-1})	V_{micro} (cm^3 g^{-1})	d_{BJH} (nm) [a]	V_{BJH} (cm^3/g) [b]
5CX	663	217	0.215	5	0.31
20CX	683	272	0.195	20	0.62
Au/20CX	632	220	0.171	19	0.62
AC [c]	1025	180	0.361	4	0.24
MWCNT [c]	285	285	0	32	1.6

[a] d_{BJH}: most frequent mesopore diameter (obtained from the desorption branch of the isotherm using the Barrett, Joyner and Halenda (BJH) method).
[b] V_{BJH}: pore volume calculated from the BJH method (corresponds to pore widths between about 4 and 90 nm).
[c] Data from Ref. [18].

The selectivities (S_i) into the different products i at time t were calculated as:

$$S_i = \frac{C_i}{v_i \cdot C_0 \cdot X}$$

where C_i is the concentration of product i (mol L^{-1}), C_0 is the initial concentration of glycerol (mol L^{-1}), X is the glycerol conversion and v_i corresponds to the moles of i produced per mol of glycerol consumed, according to the stoichiometry.

3. Results and discussion

3.1. Characterization of supports and catalysts

The main goal of the present work is to study the relationship between the textural properties of the carbon xerogels, namely the respective mesopore sizes, and the catalytic performance of gold supported on these materials for glycerol oxidation. The key variable to control those properties is the pH of the resorcinol–formaldehyde aqueous solution [19].

3.1.1. Textural properties

The textural characterization of the supports and the Au/20CX catalyst is presented in Table 1; pore size distributions profiles are depicted in Fig. 1. The BET surface area of the Au/20CX catalyst decreased only slightly compared to the unloaded carbon xerogel. Therefore, it was assumed that the textural properties of the supported gold catalysts are not significantly different from the corresponding supports.

It is evident from Table 1 and Fig. 1 that the two pHs used in sol–gel processing resulted in carbon samples with significantly different textural properties. Although the BET area is fairly similar for both samples, the 20CX support has a higher mesoporous area than 5CX, as well as a much higher average pore diameter. This difference was attributed to the lower pH used during the sol–gel processing of the parent gel (5.5 compared to 6.0 in the case of 5CX). This trend between pH and average pore size is in agreement with the observation of Job et al. [19], who reported that the average pore diameter of the final carbon material rapidly decreased with the increase of the pH used in the preparation of the parent gel. Moreover, according to literature data [25], the increase of the concentration of base in the sol–gel processing leads to carbon samples with lower mesopore volume, which also matches our results. Therefore, two carbon xerogels differing mainly in the average pore size were successfully prepared by controlling the initial pH. Additionally, it should be noticed that the use of supports with large mesopores may be favorable, particularly for liquid phase reactions, as they decrease mass transfer limitations, principally compared to the traditional microporous activated carbons.
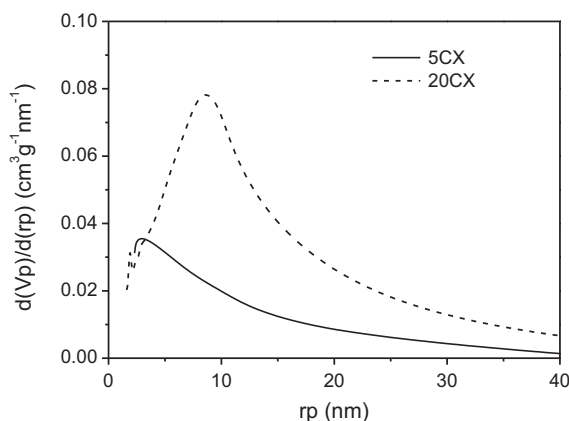
3.1.2. Surface chemistry characterization

The surface oxygen groups present on the carbon xerogels were characterized by TPD. In this technique, the total amount of the various oxygenated surface groups on carbon materials can be determined, since these groups are decomposed upon heating by releasing CO and/or CO$_2$ at different temperature ranges. Consequently, a high amount of surface oxygen is evidenced by a large release of CO and CO$_2$. Therefore, it is possible to identify and estimate the amount of the oxygenated groups on a given material by TPD experiments [23,24].

Both samples show similar surface chemistries, containing only a limited concentration of oxygenated functional groups on their surface corresponding to oxygen contents of 268 μmol g^{-1} (5CX) and 435 μmol g^{-1} (20CX). For comparison, results obtained with moderately and highly oxidized carbon materials can be found elsewhere [12,23,24,26]. Therefore, it can be concluded that both supports used in this work have a very small amount of oxygenated groups on their surface, which is important since this may influence the performance of catalysts. In fact, in a recent work, we demonstrated that the presence of surface oxygenated acid groups significantly lowers the activity of gold supported on activated carbon [12]. The surface chemistry results obtained are in agreement with those reported by Job et al. [19], who did not find any detectable absorption peak corresponding to oxygenated groups in carbon xerogels prepared in the same way as our samples, using infra-red spectroscopy.

3.1.3. Microscopy and ICP analyses

Gold nanoparticles were successfully supported on the two carbon xerogels by the sol immobilization method. Representative HRTEM images were collected in order to get information about metal particle size distributions (Fig. 2). It can be seen that small spherical metal particles are found for both catalysts prepared. The gold average particle size (d_M) and standard deviation of the studied catalysts are presented in Table 2. The protective PVA prevents efficiently the agglomeration in solution and during the supporting step by steric and polar stabilization of gold particles, leading to narrow distributions of particle sizes and to low average diameters (<5.0 nm) [27]. In fact, the gold–sol method has the advantage of predetermining the size of the gold particle, which is maintained

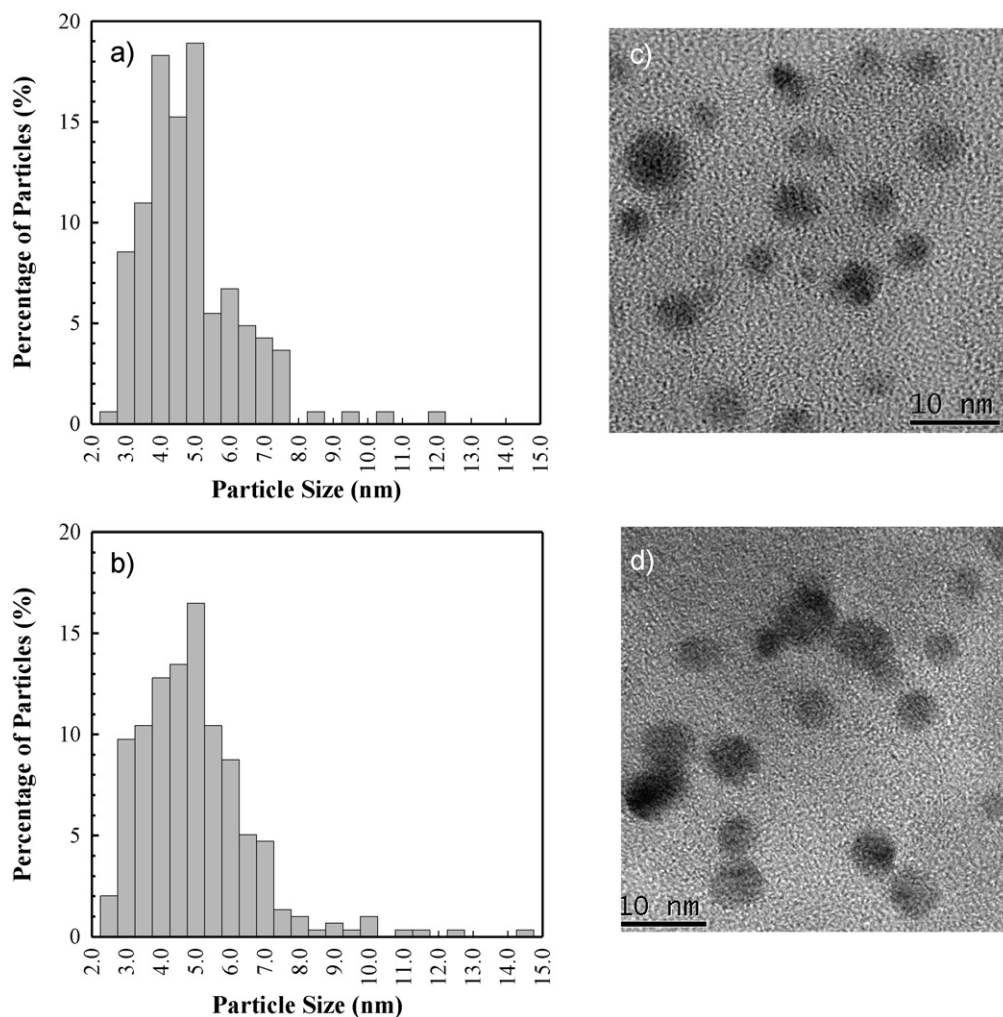**Fig. 1.** Pore size distributions obtained by the BJH method.

Fig. 2. Gold particle size distributions on (a) 5CX, (b) 20CX and HRTEM images of (c) Au/5CX and (d) Au/20CX.

during the immobilization step. Accordingly, similar average particle sizes were obtained for both catalysts prepared, independently of the different textural properties of the supports.

Table 2 also shows the metal loadings of the catalysts. The gold content obtained by ICP analysis is lower than the nominal, which indicates that a fraction of gold present in the aqueous solution was not deposited on the supports. In fact, it should be noticed that the adsorption of gold sols on the carbon xerogels was difficult, particularly when concentrations of gold in solution become low, resulting in fairly high immobilization times (approximately 3 weeks). A similar situation was observed by Porta et al. [27] when using PVA sols on oxides. This behavior can be due to the absence of significant concentrations of functional groups on the surface of carbon xerogels [28], as mentioned in Section 3.1.2. As a result, the hydrophobic surface of carbon xerogels has a very limited affinity to the gold hydrosol. In spite of the low efficiency, it was possible to obtain a gold loading of approximately 0.6 wt% for both samples.

Table 2
Average crystallite size and metal content of the studied catalysts.

Catalyst	Metal loading (wt%) [ICP]	d_M (nm) [TEM]	Standard deviation (nm)
Au/5CX	0.62 ± 0.02	4.6	1.5
Au/20CX	0.59 ± 0.02	4.7	1.7

3.2. Catalytic studies

The principal aim of this study is to evaluate possible correlations between activity and/or selectivity of the Au/CX catalysts and the textural properties of the support.

Fig. 3 shows the evolution of glycerol conversion in the presence of the gold catalysts prepared on the two carbon xerogels. It can be observed that gold supported on CXs are efficient catalysts for glycerol oxidation. The amount of gold eventually leached during reactions was measured in a UNICAM 939/959 atomic absorption spectrometer using the remaining solution after 5 h of reaction. In these determinations, no gold was detected, and so gold particles seem to have a strong interaction with both xerogel supports, which prevents leaching. Although Au/5CX shows a better performance, the turnover frequencies (TOFs) calculated after 2 h of reaction are fairly high and similar for both catalysts, as reported in Table 3. On the other hand, a possible slightly higher TOF for Au/5CX can be noticed, but the errors involved do not allow definitive conclusions. It is well known that the catalytic activity is largely influenced by the gold particle size, the catalysts with smaller gold particles being more active [9,20,29,30]. However, Au/5CX and Au/20CX have almost identical average particle sizes (4.6 nm and 4.7 nm, respectively), and therefore similar activities were expected.

Mass transfer resistances inside the porous network of the support can be limiting, and then influence strongly the performance of the catalysts. As the catalysts tested in this work show different
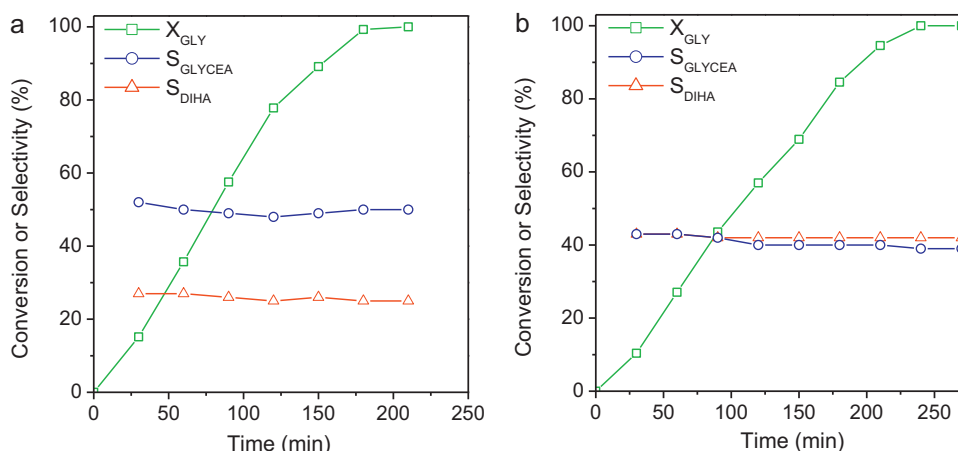
Fig. 3. Conversion of glycerol (X_{GLY}) and selectivities to main products (S_{GLYCEA} and S_{DIHA}) as a function of time using (a) Au/5CX and (b) Au/20CX in glycerol oxidation. Reaction conditions: 60 °C, $p_{O_2} = 3$ bar, 150 mL of glycerol 0.3 M, catalyst amount = 700 mg, NaOH/glycerol = 2 mol/mol.

pore sizes, the influence of intraparticle diffusion was assessed on the basis of the Weisz-Prater criterion [31]. The calculations of the Weisz modulus Φ indicated that the process is not significantly influenced by intraparticular diffusion, under the conditions used.

The putative small difference in the activities of the two catalysts can be due to to the electrical resistivity of the materials. In fact, we suggested that supports that allow a high electronic mobility, and therefore have a low electrical resistivity, promote the catalytic performance by the enhancement of the regeneration of hydroxide ions [12]. Job et al. [19] showed that the electrical resistivity of carbon xerogels strongly depends on the carbon texture and decreases with the decrease of the average pore diameter. Accordingly, the support of Au/5CX ($d_{BJH} = 5$ nm) has a lower electrical resistivity than that of Au/20CX ($d_{BJH} = 20$ nm) and consequently the former catalyst enhances the mobility of electrons, which is in agreement with the possible slightly higher activity observed.

While various studies have demonstrated the influence of gold particle size on the catalytic activity, the selectivity does not seem to correlate directly with the size of nanoparticles [2,7,20,29]. Indeed, Villa et al. concluded that during glycerol oxidation in the presence of gold on MgAl$_2$O$_4$ the selectivity of the reaction was only partially determined by the gold particle size [15]. On the other hand, an increasing number of recent studies suggest that the textural and chemical properties of the support influence directly the selectivities attained in the glycerol oxidation reaction [12,15–18]. Then, the effect of the porous texture of the CX supports on the distribution of products was also evaluated. The selectivities obtained in the presence of the two catalysts are compared at constant glycerol conversion ($X_{GLY} = 90\%$) in Table 3. It is important to mention that the selectivities are practically independent of time or glycerol conversion, varying only slightly during the reaction, as can be seen in Fig. 3, where the selectivities to the main reaction products are also plotted as a function of time.

For both catalysts tested the main reaction products are DIHA and GLYCEA, which correspond to valuable oxygenated compounds. Accordingly, a high total selectivity to these products of commercial interest was obtained (73% for Au/5CX and 82% for Au/20CX). However, it can be observed that there is an important variation in the distributions obtained, depending on the carbon xerogel used. In fact, whereas the Au/5CX catalyst favors the formation of GLYCEA (selectivity of 48% at $X_{GLY} = 90\%$), Au/20CX leads to DIHA as the main product (selectivity of 42% at $X_{GLY} = 90\%$). The difference on the selectivities to this latter compound is especially remarkable, since it is only 25% in the presence of Au/5CX. In addition to the products depicted in Table 3, a small amount of oxalic acid was detected in the case of Au/5CX (sum of the selectivities presented in Table 3 lower than 1), whose formation is due to the subsequent oxidation of glyceric acid [15]. Beyond oxalic acid, a larger amount of TARTA was also obtained in the case of Au/5CX (see Table 3). This can be explained by the presence of narrow pores in this support, which can lead to an easier over-oxidation of the primary products [4].

In this study, catalysts with similar gold average particle sizes, metal loadings and support chemical properties were successfully prepared. Therefore, the disparities in the selectivities observed in Fig. 3 seem to be related almost exclusively to the differences in the textural properties. Indeed, an increase of the most frequent pore diameter from 5 to 20 nm leads to an enhancement of the selectivity to DIHA from 25% to 42% and to a decrease of the selectivity to GLYCEA. Wide pores apparently favor the formation of DIHA, whereas narrow pore sizes lead to the preferential formation of glyceric acid. In order to investigate more deeply the relationship between pore size and selectivity, a comparison with other carbon materials previously studied as supports [18], namely multi-walled carbon nanotubes (MWCNT) and activated carbon (AC), was also carried out.

Table 3

Influence of the textural properties of the support on the activities and selectivities to dihydroxyacetone (DIHA), glyceric acid (GLYCEA), glycolic acid (GLYCOA) and tartronic acid (TARTA) for the Au/CX catalysts.

Catalyst	$t = 120$ min		$X_{GLY} = 90\%$			
	X_{GLY} (%)	TOF × 10^{-3} (h^{-1}) [a]	S_{DIHA} (%)	S_{GLYCEA} (%)	S_{GLYCOA} (%)	S_{TARTA} (%)
Au/5CX	78	2.9 ± 0.9	25	48	20	5
Au/20CX	57	2.5 ± 0.9	42	40	17	1

[a] TOF (h^{-1}) = (mole of glycerol converted after 2 h)/(reaction time (= 2 h) × mole of gold active sites); the amount of gold active sites were calculated from $(6 \times y \times n_s \times W_{cat})/(d_M \times \rho \times N)$, where y and d_M are the gold weight fraction (from ICP) and the average particle diameter (from TEM), respectively; ρ and n_s are the density of gold and the number of gold atoms per unit of area, respectively; W_{cat} is the catalyst mass used in the experiments (0.7 g); and N is the Avogadro number; errors of TOF were calculated on the basis of errors related to the measurements of gold loadings and standard deviations of particle size distributions.
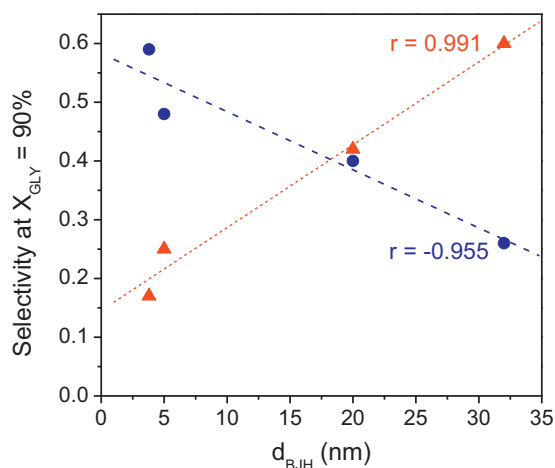
Fig. 4. Correlations between selectivities to DIHA (▲) and GLYCEA (●) and the most frequent mesopore size of carbon supports (calculated by the BJH method). Reaction conditions: 60 °C, p_{O_2} = 3 bar, 150 mL of glycerol 0.3 M, catalyst amount = 700 mg, NaOH/glycerol = 2 mol/mol.

It was recently reported that gold supported on MWCNT lead to a selectivity of 60% to DIHA and only 26% to GLYCEA [18]. This catalyst has mesopore sizes largely distributed with a mode of 32 nm. On the contrary, when gold is supported on activated carbon (AC), which corresponds to a support with micropores and small mesopores, an opposite distribution of products is obtained (18% to DIHA and 62% to GLYCEA) [18]. This is in accordance with the trend observed for the Au/CX catalysts, which make us to believe that the textural properties of the supports are the main responsible for the different distributions of products observed. For comparison, some textural properties of MWCNT and AC are shown on Table 1. It is also important to mention that all the carbon supports of this work have a similar (very limited) amount of oxygenated groups on their surface; only in this way the comparison between catalysts is possible [12]. Additionally, the gold average particle size varies only slightly (from 4.6 nm for Au/5CX to 6.8 nm for the Au/AC catalyst) and no relationship between this parameter and the product distribution was observed. In fact, gold supported on MWCNT catalysts with variable average particle sizes (from 3.2 nm to 6.5 nm) were tested in glycerol oxidation and no significant differences in the selectivities were observed [32]. All these results suggest that the pore sizes of the support play an important role on the distribution of the products.

In Fig. 4, the selectivities to DIHA and GLYCEA obtained in the presence of gold supported on different carbon materials (AC, CXs and MWCNT) were plotted as a function of the most frequent mesopore diameter. Significant correlations are noticed, particularly in the case of DIHA. Accordingly, an increase in the mesopore sizes of the support leads to an increase in the selectivity to DIHA and a decrease to GLYCEA. Nevertheless, this feature of the support seems to influence more the amount of DIHA obtained. It was suggested that the oxidation of the secondary alcohol group (DIHA) can be due to a different adsorption mode [15,18]. The formation of DIHA can require the binding of the glycerol molecule in a conformation that needs more space and therefore is favored by supports with large pores.

It should be noticed that DIHA is not stable under alkaline conditions, and therefore the conditions used during the reaction are not suitable to store DIHA-containing mixtures for long periods of time. In order to avoid DIHA transformation reactions, the pH of the solution must be lowered to a value around 3 [32].

As a result, it seems that the distribution of products can be tuned within certain limits by the adequate choice of the support. Therefore, carbon xerogel appears to be a useful material since their porous textural features can be easily tailored to meet specific requirements.

4. Conclusions

The mesopore size distribution of carbon xerogels used as support of gold catalysts in glycerol oxidation strongly influences the selectivity. Wide mesopores favor the formation of dihydroxyacetone, whereas narrow pores lead to the preferential formation of glyceric acid. The same trend was observed with gold supported on activated carbon and multi-walled carbon nanotubes. Therefore, the type of carbon support plays an important role in the distribution of the products and it seems possible to tune the selectivity. In this way, carbon xerogel is an advantageous material since its average pore size can be easily adjusted in a controllable way during the preparation process.

Acknowledgements

References

[1] C.H.C. Zhou, J.N. Beltramini, Y.X. Fan, G.Q.M. Lu, Chem. Soc. Rev. 37 (2008) 527–549.
[2] B. Katryniok, H. Kimura, E. Skrzynska, J.-S. Giradon, P. Fongarland, M. Capron, R. Ducoulombier, N. Mimura, S. Paul, F. Dumeignil, Green Chem. 13 (2011) 1960–1979.
[3] M. Pagliaro, R. Ciriminna, H. Kimura, M. Rossi, C. Della Pina, Angew. Chem. Int. Ed. 46 (2007) 4434–4440.
[4] P. McMorn, G. Roberts, G.J. Hutchings, Catal. Lett. 63 (1999) 193–197.
[5] R. Garcia, M. Besson, P. Gallezot, Appl. Catal. A 127 (1995) 165–176.
[6] E.G. Rodrigues, S.A.C. Carabineiro, X. Chen, J.J. Delgado, J.L. Figueiredo, M.F.R. Pereira, J.J.M. Órfão, Catal. Lett. 141 (2011) 420–431.
[7] N. Dimitratos, A. Villa, C.L. Bianchi, L. Prati, M. Makkee, Appl. Catal. A 311 (2006) 185–192.
[8] H. Kimura, K. Tsuto, T. Wakisaka, Y. Kazumi, Y. Inaya, Appl. Catal. A 96 (1993) 217–228.
[9] F. Porta, L. Prati, J. Catal. 224 (2004) 397–403.
[10] M. Besson, P. Gallezot, Catal. Today 57 (2000) 127–141.
[11] L. Prati, M. Rossi, J. Catal. 176 (1998) 552–560.
[12] E.G. Rodrigues, M.F.R. Pereira, X. Chen, J.J. Delgado, J.J.M. Órfão, J.Catal. 281 (2011) 119–127.
[13] S. Demirel, K. Lehnert, M. Lucas, P. Claus, Appl. Catal. B 70 (2007) 637–643.
[14] S. Demirel, P. Kern, M. Lucas, P. Claus, Catal. Today 122 (2007) 292–300.
[15] A. Villa, A. Gaiassi, I. Rossetti, C.L. Bianchi, K. van Benthem, G.M. Veith, L. Prati, J. Catal. 275 (2010) 108–116.
[16] B.N. Zope, D.D. Hibbitts, M. Neurock, R.J. Davis, Science 330 (2010) 74–78.
[17] L. Prati, A. Villa, C.E. Chan-Thaw, R. Arrigo, D. Wang, D.S. Su, Faraday Discuss. 152 (2011) 353–365.
[18] E.G. Rodrigues, M.F.R. Pereira, J.J. Delgado, X. Chen, J.J.M. Órfão, Catal. Commun. 16 (2011) 64–69.
[19] N. Job, R. Pirard, J. Marien, J.-P. Pirard, Carbon 42 (2004) 619–628.
[20] S. Demirel-Gülen, M. Lucas, P. Claus, Catal. Today 102-103 (2005) 166–172.
[21] G.J. Hutchings, S. Carrettin, P. Landon, J.K. Edwards, D. Enache, D.W. Knight, Y.J. Xu, A.F. Carley, Top. Catal. 38 (2006) 223–230.
[22] Y. Onal, S. Schimpf, P. Claus, J. Catal. 223 (2004) 122–133.
[23] J.L. Figueiredo, M.F.R. Pereira, M.M.A. Freitas, J.J.M. Órfão, Carbon 37 (1999) 1379–1389.
[24] J.L. Figueiredo, M.F.R. Pereira, M.M.A. Freitas, J.J.M. Órfão, Ind. Eng. Chem. Res. 46 (2007) 4110–4115.
[25] T. Yamamoto, A. Endo, T. Ohmori, M. Nakaiwa, Carbon 43 (2005) 1231–1238.
[26] N. Mahata, M.F.R. Pereira, F. Suárez-García, A. Martínez-Alonso, J.M.D. Tascón, J.L. Figueiredo, J. Colloid Interface Sci. 324 (2008) 150–155.
[27] F. Porta, L. Prati, M. Rossi, S. Coluccia, G. Martra, Catal. Today 61 (2000) 165–172.
[28] M. Comotti, C.D. Pina, R. Matarrese, M. Rossi, A. Siani, Appl. Catal. A 291 (2005) 204–209.
[29] W.C. Ketchie, Y.-L. Fang, M.S. Wong, M. Murayama, R.J. Davis, J. Catal. 250 (2007) 94–101.
[30] S. Carrettin, P. McMorn, P. Johnston, K. Griffin, C.J. Kiely, G.J. Hutchings, Phys. Chem. Chem. Phys. 5 (2003) 1329–1336.
[31] G.F. Froment, K.B. Bischoff, Chemical Reactor Analysis and Design, 2nd ed., Wiley, New York, 1990.
[32] E.G. Rodrigues, S.A.C. Carabineiro, J.J. Delgado, X. Chen, M.F.R. Pereira, J.J.M. Órfão, J. Catal. (2011), doi:10.1016/j.jcat.2011.09.016.